J Mater Sci (2011) 46:7633–7638
DOI 10.1007/s10853-011-5741-z

Amorphous phase formation in $Al_{80}Fe_{10}M_{10}$ (M = Ni, Ti, and V) ternary systems by mechanical alloying

M. Tavoosi · F. Karimzadeh · M. H. Enayati · S.-H. Joo · H. S. Kim

Received: 18 April 2011 / Accepted: 22 June 2011 / Published online: 7 July 2011

Abstract In this study, the amorphous phase formation in $Al_{80}Fe_{10}M_{10}$ (M = Ti, V, Ni) (at.%) ternary systems during mechanical alloying has been investigated. The milled samples were characterized using X-ray diffraction and differential thermal analyses. A thermodynamic analysis of the amorphous phase formation was performed for these systems using the Miedema model. The obtained results demonstrate that amorphous phases can be formed during the mechanical alloying process of the $Al_{80}Fe_{10}M_{10}$ (M = Ti, V, Ni) ternary systems. The produced amorphous alloys exhibit one-stage crystallization during heating, which is amorphous to the $Al_{13}Fe_4$ intermetallic phases. The thermal stability of the produced amorphous phases decreases in the order of $Al_{80}Fe_{10}Ti_{10} > Al_{80}Fe_{10}Ni_{10} > Al_{80}Fe_{10}V_{10}$.

Introduction

Structural materials with high-specific strength are consistently of considerable interest to the transportation and aviation industries [1, 2]. Thus, the development of an Al-based metallic glass is eagerly awaited in these industries due to its perceived benefits [3]. A new class of Al-base alloys, which has received a great deal of attention over the last few years, is amorphous as well as nanocrystalline ones [4–8]. It is predicted that the strength of the light weight aluminum alloys can be significantly enhanced from approximately 450–600 MPa in age hardened conditions to over 1500 MPa in amorphous or nanocrystalline dispersed amorphous matrix aluminum-based alloys [9–11]. Among various Al alloys, Al–Fe systems are of technological interest because of their advantageous properties, in particular a high-specific-strength, -stiffness, good strength at intermediate temperatures, and excellent corrosion resistance at elevated temperatures under oxidizing and carburizing atmospheres [1, 11]. However, the alloys in Al rich side of Al–Fe alloying system have low glass forming ability and the stability of glass phase in this alloying systems are so low. By addition of one or more alloying elements to these systems, it is expected that the glass forming ability and the thermal stability of amorphous phase can be improved [4, 12].

The mechanical alloying (MA) process is a convenient solid state synthesis alternative to melt spinning and similar rapid quenching techniques that are used to develop amorphous alloys with metastable microstructures at ambient temperatures. In this process, continuous welding and fracture of the input powders occurs, and the constant bombardment of the powders by strong balls increases the defect concentrations in the alloy and increases the free energy of the solid solution, which is formed during the initial stages of milling. Once the free energy of the powders rises above the free energy of the amorphous phase, the amorphous phase can be formed [8, 9].

It has been established that phases with negative Gibbs free energy at room temperature can be formed from elemental powder mixtures during the MA process. Hence, the thermodynamic properties of the alloys are very important for the evaluation and understanding of the possible range

M. Tavoosi · F. Karimzadeh · M. H. Enayati
Department of Material Engineering, Nanotechnology and Advanced Material Institute, Isfahan University of Technology (IUT), 84156-83111 Isfahan, Iran

M. Tavoosi · S.-H. Joo · H. S. Kim (✉)
Department of Materials Science and Engineering, POSTECH (Pohang University of Science and Technology), Pohang 790-784, Korea
e-mail: hyoungseopkim@gmail.com

for glass forming compositions and thermal stability in alloying systems [6, 13]. In general, the thermodynamic properties of the alloys can be obtained through experimental measurements. However, it is not always possible to perform experimental measurements for multi-component alloys due to technological difficulties, expense, and time use. Therefore, using theoretical predictions and extrapolation are significant and effective approaches for obtaining the thermodynamic properties of alloys, especially for multi-component systems.

In this study, the fabrication and characterization of amorphous $Al_{80}Fe_{10}M_{10}$ (M = Ti, V, Ni) alloys were investigated using the MA process for the elemental powder mixtures. The structural changes during the MA process and thermal behavior of the milled products were studied using X-ray diffraction (XRD) and differential thermal analysis (DTA) methods. The method based in the Miedema theory was also used to calculate the mixing enthalpies of the systems.

Thermodynamic description

Generally, the Gibbs free energy of an alloy phase can be calculated using $\Delta G = \Delta H - T\Delta S$, where ΔH and ΔS are the enthalpy and entropy terms, respectively [12]. For a ternary alloy system with constituents of A, B, and C, ΔS can be calculated as follows:

$$\Delta S^S = -R(x_A \ln x_A + x_B \ln x_B + x_C \ln x_C), \quad (1)$$

where R is the gas constant, and x_A, x_B, and x_C are the atomic concentrations of metals A, B, and C, respectively.

According to the Miedema model, the formation enthalpy of a solid solution is given by [14, 15]:

$$\Delta H_{\text{sol}} = \Delta H_{\text{chem}} + \Delta H_{\text{e}} + \Delta H_{\text{struct}}, \quad (2)$$

where ΔH_{chem}, ΔH_{e}, and ΔH_{struct} are the chemical contribution, elastic, or atomic size mismatch contribution, and structural contribution, respectively.

From the Miedema semi-empirical model [16], in the melting or amorphous state, the elastic and structural contributions are absent; thus, the formation enthalpy of liquid (ΔH_{liq}), glass (ΔH_{amor}), and intermetallic compounds (ΔH_{inter}) can be readily calculated as follows:

$$\Delta H^{\text{liq}} = \Delta H^{\text{chem}}(\text{liq}), \quad (3)$$

$$\Delta H^{\text{amor}} = \Delta H^{\text{chem}}(\text{amor}) + 3.5\sum_{i=1}^{n} x_i \cdot T_{\text{m},i}, \quad (4)$$

$$\Delta H^{\text{inter}} = \Delta H^{\text{chem}}(\text{inter}), \quad (5)$$

where $\Delta H^{\text{chem}}(\text{liq})$, $\Delta H^{\text{chem}}(\text{amor})$, and $\Delta H^{\text{chem}}(\text{inter})$ are the chemical enthalpy of the liquid state, amorphous state, and intermetallic compounds, respectively. $T_{\text{m},i}$ is the melting temperature of the component i and ΔH^{chem} is the solution enthalpy of A in B:

$$\Delta H^{\text{chem}} = x_A x_B (f_B^A \Delta H_{\text{sol}}^{A \text{ in } B} + f_A^B \Delta H_{\text{sol}}^{B \text{ in } A}), \quad (6)$$

$$\Delta H_{\text{sol}}^{A \text{ in } B} = 2V_A^{\frac{2}{3}} \left[-P(\Delta\Phi)^2 + Q\left(\Delta n_{\text{ws}}^{\frac{1}{3}}\right)^2 \right] \Big/ \left[(n_{\text{ws}})_A^{-\frac{1}{3}} + (n_{\text{ws}})_B^{-\frac{1}{3}} \right], \quad (7)$$

$$f_j^i = c_j \left[1 + k(c_i \cdot c_j)^2 \right], \quad (8)$$

$$c_j = x_j V_j^{\frac{2}{3}} / \left(x_j V_j^{\frac{2}{3}} + x_i V_i^{\frac{2}{3}} \right), \quad (9)$$

where V, Φ, and n_{ws} are the molar volume, work function, and electron density of the constituents, respectively. P and Q are empirical constants with the same value for widely different metal combinations. The constant k is taken to be five for a short-range order and eight for a long-range order.

To calculate the formation enthalpies of ternary systems, the Miedema theory presents a simple method based on that used to calculate binary systems [17–19]. A predigestion is employed which turns a ternary problem into three binary problems; it can be described as:

$$\Delta H_{ABC} = \Delta H_{A \text{ in } B}^C + \Delta H_{B \text{ in } C}^A + \Delta H_{A \text{ in } C}^B, \quad (10)$$

where ΔH_{ABC} is the standard formation enthalpy of the ternary intermetallic compounds or ternary amorphous alloys. $\Delta H_{A \text{ in } B}^C$ is the heat of the solution of metal A in metal B, regardless of the effect of metal C: that is, the method for calculating $\Delta H_{A \text{ in } B}^C$, $\Delta H_{B \text{ in } C}^A$, and $\Delta H_{A \text{ in } C}^B$ for ternary systems is similar to that for binary systems.

Experimental

The powders of Al (99% purity), Fe (99.9% purity), Ti (99% purity), Ni (99% purity), and V (99.9% purity) were used as raw materials. The elemental powders with composition of $Al_{80}Fe_{10}M_{10}$ (M = Ni, Ti, V) (at.%) were mechanically alloyed in a planetary ball mill in an argon atmosphere. The MA process was performed in a steel container at room temperature. The rotation speed was 400 rpm and the ball to powder ratio was 10:1. One wt% stearic acid powder was used as the process control agent (PCA). An XRD using a diffractometer with Cu Kα radiation ($\lambda = 0.15406$ nm; 40 kV; Philips) was used to follow the structural changes of the powders during milling and the subsequent annealing. A DTA was also conducted to study the thermal stability of the produced amorphous alloy using a Reometric™ STA 1500 analyzer. The samples were placed in Al_2O_3 pans and heated in a dynamic argon

atmosphere up to 1000 °C at a constant heating rate of 20 °C/min.

Results and discussion

Formation enthalpy of amorphous phase in Al–Fe–M (M = Ni, Ti, V) ternary systems

The thermodynamic properties of alloys are very important for the evaluation of the glass forming capability and thermal stability in alloying systems. In this study, the Miedema theory was used to calculate the thermodynamic properties (mixing enthalpies) of the systems.

The formation enthalpies of the amorphous phase of the whole composition for Al–Fe–M (M = Ni, Ti, V) ternary systems are shown in Fig. 1. The contour maps for the formation enthalpies of the amorphous phases depend not only on the composition but also on the atomic interactions between the elements, as shown in Table 1. The highest formation enthalpy (−36 kJ/mol) in the Al–Fe–Ni system is seen at $Al_{50}Ni_{50}$ in Fig. 1a, which monotonously decreases to 0 kJ/mol at the Al, Fe, and Ni corners. However, similar to the Al–Fe–Ni system, the highest formation enthalpy (−50 kJ/mol) in the Al–Fe–Ti in Fig. 1b is achieved at $Al_{50}Ti_{50}$, and the maximum value of formation enthalpy (−40 kJ/mol) in Al–Fe–V in Fig. 1c is seen at $Al_{30}Fe_{40}V_{40}$. The difference of the formation enthalpies in the contour maps for these systems can be attributed to the differences in the atomic interactions between the constituent elements in each alloying system; the different Al–Fe, Al–Ti, Al–Ni, Al–V, Fe–Ti, Fe–Ni, and Fe–V atomic interactions are seen in Table 1.

The MA of $Al_{80}Fe_{10}M_{10}$ (M = Ni, Ti, V)

Reactions with negative changes in the Gibbs free energy at room temperature can occur in the elemental powder

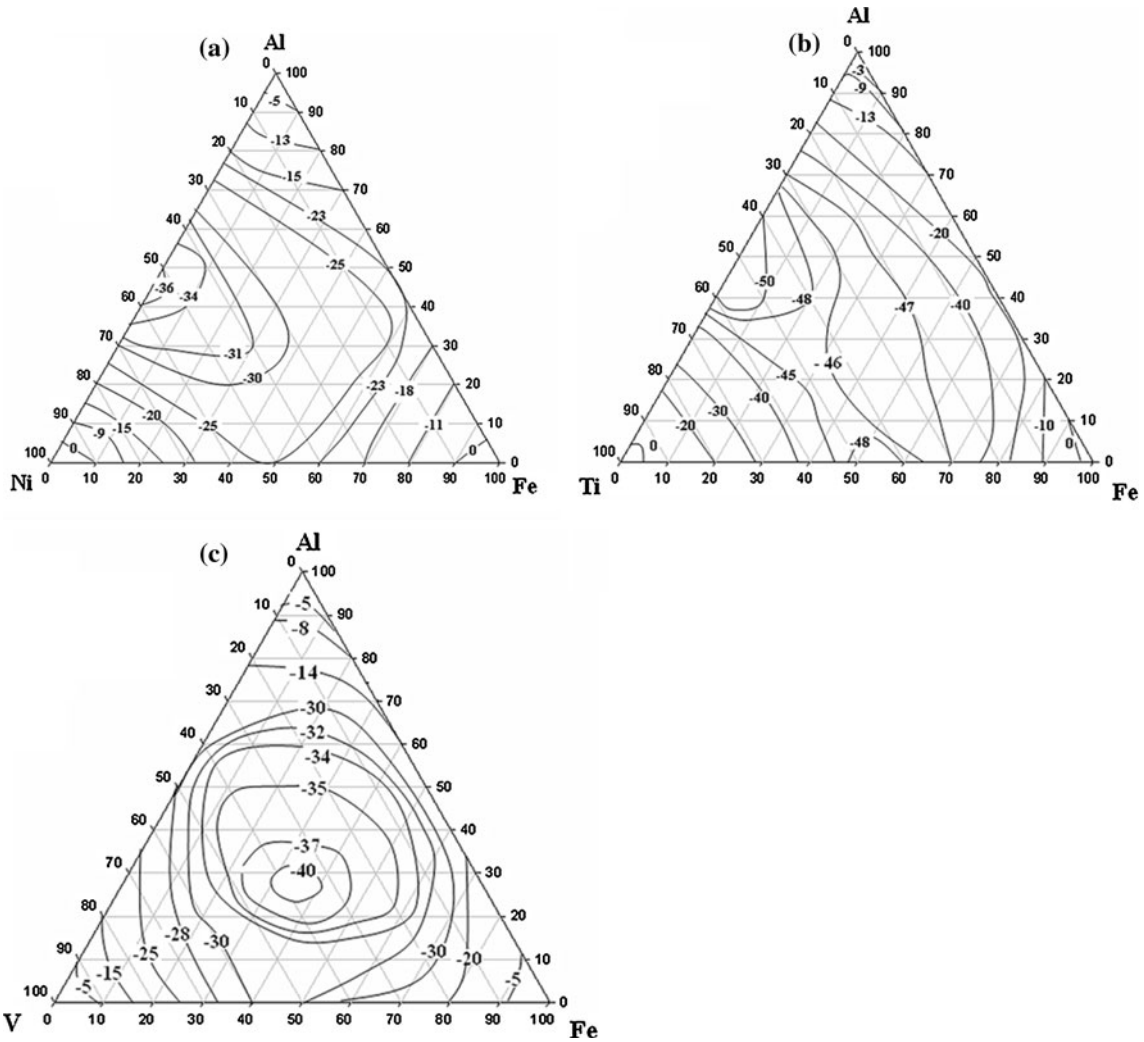

Fig. 1 The calculated mixing enthalpies (kJ/mol) of the entire composition for **a** Al–Fe–Ni, **b** Al–Fe–Ti, and **c** Al–Fe–V ternary systems

Table 1 Heat of solution (kJ/mol) for several binary alloying systems calculated using the Miedema model

Solution	Solvent				
	Al	Fe	Ni	V	Ti
Al	–	–95	–148	–112	–173
Fe	–76	–	–98	–116	–150
Ni	–112	–93	–	150	–210
V	–100	–128	–175	–	–114
Ti	–181	–195	–288	–98	–

mixtures during the MA process [4]. Using the data from Fig. 1, the values of the changes in the enthalpy and Gibbs free energy due to the amorphous phase formation for $Al_{80}Fe_{10}M_{10}$ (M = Ni, Ti, V) are presented in Table 2. According to these results, there is a thermodynamic driving force to form amorphous phases in each $Al_{80}Fe_{10}M_{10}$ (M = Ti, V, Ni) ternary system. The effectiveness of the M elements in forming an amorphous phase (according to the thermodynamic aspects) decreases in the order of Ti > Ni > V, suggesting that the bonding nature between Al, Fe, and the other constituent elements decreases in the same order as shown in Table 1.

The XRD patterns of the $Al_{80}Fe_{10}Ni_{10}$ powder mixtures after various MA processing periods are shown in Fig. 2. In the early stage of the MA process, only the broadening of the Al, Fe, and Ni peaks accompanied by remarkable decreases in their intensities occurred as a result of the refinement of the crystalline sizes and increments of the lattice strains. Increasing milling time to 5 h led to the disappearance of the Fe and Ni peaks, while the Al (111) peak shifted to higher angles as shown in Fig. 3. This is a result of the dissolution of Fe and Ni in the Al lattice.

By increasing the milling time, three peaks corresponding to the decagonal phases (D-phase) [20, 21] are observed in the XRD patterns and confirmed using the TEM analysis. The observed D-phase peaks demonstrate the formation of the D-phase from the solid solution. After 15 h of the MA process, the D-phase transformed to (Ni,Fe)Al intermetallic phase. Analyses of the XRD patterns in Fig. 2 reveal that the (Ni,Fe)Al intermetallic compound formed from the D-phase during milling could be amorphized by further milling (after 25 h). Hence, the structural changes in the $Al_{80}Fe_{10}Ni_{10}$ system during the MA process can be written as:

Elemental powder → solid solution → D-phases
→ (Ni,Fe)Al intermetallic
→ amorphous phase

Figures 4 and 5 show the XRD patterns of the $Al_{80}Fe_{10}Ti_{10}$ and $Al_{80}Fe_{10}V_{10}$ powder blends subjected to the MA process, respectively. In the initial stages of milling in these systems (similar to $Al_{80}Fe_{10}Ni_{10}$), Fe, V, and Ti dissolve in the Al lattice and the Al solid solution is formed.

Table 2 The value of changes in the mixing enthalpy and Gibbs free energy for $Al_{80}Fe_{10}M_{10}$ (M = Ni, Ti, V) calculated using the Miedema model

	$Al_{80}Fe_{10}Ni_{10}$ (kJ/mol)	$Al_{80}Fe_{10}Ti_{10}$ (kJ/mol)	$Al_{80}Fe_{10}V_{10}$ (kJ/mol)
ΔH_{298}^{amor}	–13.3	–19	–11.4
ΔG_{298}^{amor}	–14.9	–20.6	–13

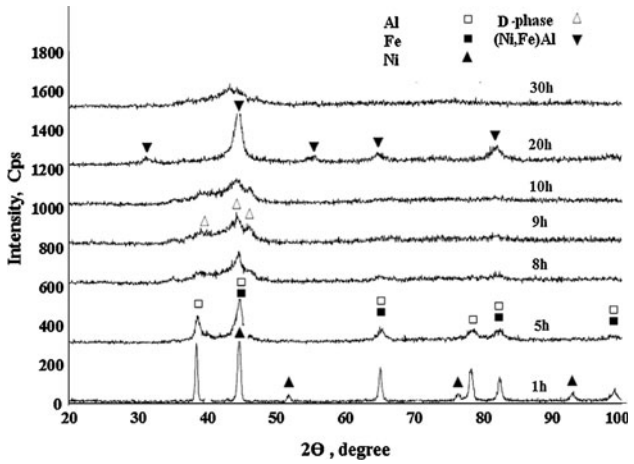

Fig. 2 XRD patterns of the $Al_{80}Fe_{10}Ni_{10}$ powder mixtures milled for different time periods

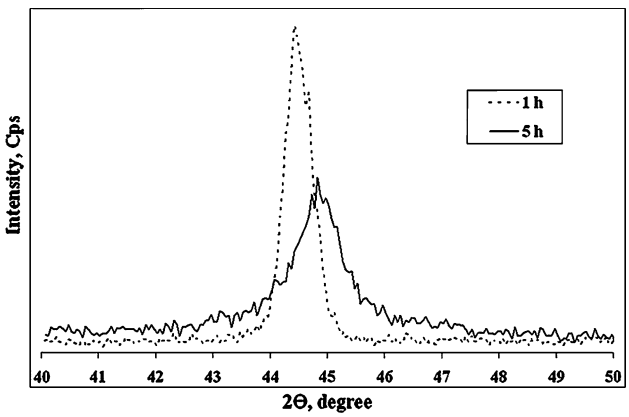

Fig. 3 Shifting of the Al (111) XRD peak after 1 and 5 h of milling $Al_{80}Fe_{10}Ni_{10}$ powder mixtures

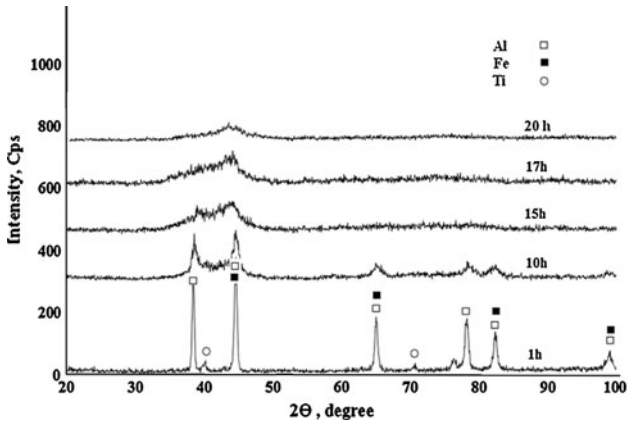

Fig. 4 XRD patterns of the $Al_{80}Fe_{10}Ti_{10}$ powder mixture milled for various time periods

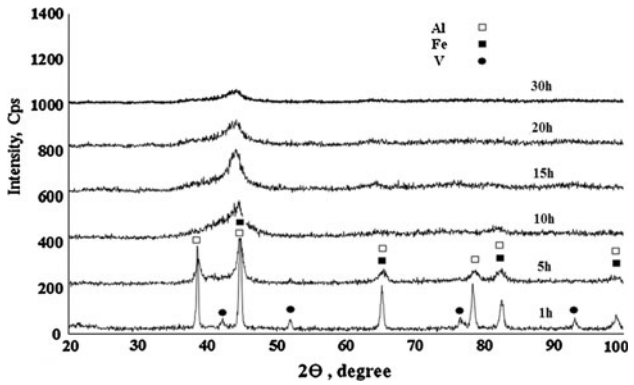

Fig. 5 XRD patterns of the $Al_{80}Fe_{10}V_{10}$ powder mixture milled for various time periods

A broad halo in the $2\theta = 30$–50° range due to the partial amorphization of the Al-rich solid solution appears in the XRD pattern after 10 h of the MA process. Increasing the milling time to 20 and 30 h leads to complete amorphization of the solid solutions. We also confirmed the fully amorphous structures using a normal TEM technique (although not shown here). However, it should be noted that there can be very tine nanocrystals of a few nanometer size or short/medium range ordered regions, which cannot be detected using the normal TEM technique. The phase subsequence of the $Al_{80}Fe_{10}Ti_{10}$ and $Al_{80}Fe_{10}V_{10}$ systems during the MA process can be written as:

Elemental powder → solid solution
→ amorphous phase

Thermal stability

In order to study the thermal stability of the produced amorphous phase, the sample was examined using DTA

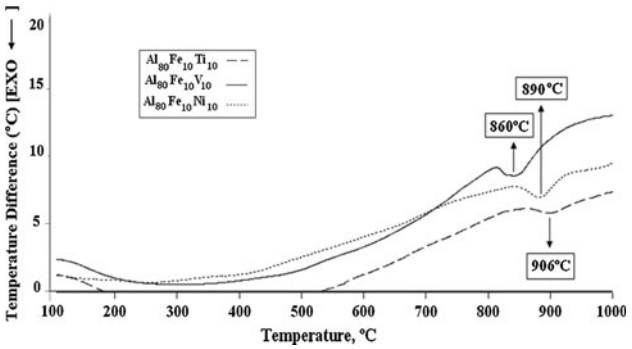

Fig. 6 The DTA heating traces of the $Al_{80}Fe_{10}M_{10}$ (M = Ni, Ti, V) amorphous alloys at a constant heating rate of 20 °C/min

under continuous heating conditions. Figure 6 shows the DTA heating traces of the $Al_{80}Fe_{10}M_{10}$ (M = Ni, Ti, V) amorphous alloys at a constant heating rate of 20 °C/min. As seen in this figure, only one exothermic peak appears in the DTA curves. To analyze the crystallization process responsible for the exothermic peak, the produced amorphous samples were annealed in an argon atmosphere at 950 °C for 20 min. The XRD patterns of the $Al_{80}Fe_{10}Ti_{10}$ amorphous phase after annealing at 950 °C are presented in Fig. 7. As seen in this figure, the sample annealed at 950 °C is primarily composed of the $Al_{13}Fe_4$ intermetallic phase (50-0797 ICDD card). Therefore, the exothermic peak in Fig. 6 should be attributed to the precipitation of the $Al_{13}Fe_4$ phase from the amorphous phase. Although the total transformation sequences of the $Al_{80}Fe_{10}Ti_{10}$, $Al_{80}Fe_{10}V_{10}$, and $Al_{80}Fe_{10}Ni_{10}$ amorphous alloys are similar, i.e., they are one-stage processes, the crystallization temperatures in these three systems differ to each other. As shown in Fig. 6, the crystallization temperatures of the $Al_{80}Fe_{10}Ti_{10}$, $Al_{80}Fe_{10}Ni_{10}$, and $Al_{80}Fe_{10}V_{10}$ amorphous alloys are 906, 890, and 860 °C, respectively.

Indeed, the crystallization temperatures of the amorphous alloys are usually dominated by an attractive interaction of the constituent atoms and are dependent on the

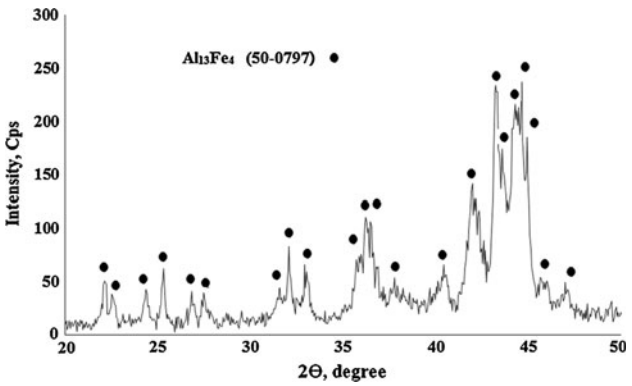

Fig. 7 The XRD pattern of the amorphous $Al_{80}Fe_{10}Ti_{10}$ alloy annealed at 950 °C for 20 min

bonding nature between the elements' atoms in the amorphous alloys. The different atomic interactions between the alloying elements in the amorphous systems lead to different changes in the Gibbs free energy and formation enthalpy of the amorphous phases in these systems. These points, according to Tables 1 and 2, demonstrate that the thermal stabilities of the produced amorphous phases decrease in the order of $Al_{80}Fe_{10}Ti_{10} > Al_{80}Fe_{10}$ $Ni_{10} > Al_{80}Fe_{10}V_{10}$.

Conclusion

This study has presented the structural changes in $Al_{80}Fe_{10}M_{10}$ (M = Ni, Ti, V) ternary alloy systems during the MA process. The results showed that amorphous phases can be formed during the MA process in $Al_{80}Fe_{10}M_{10}$ (M = Ni, Ti, V). The crystallization process of the produced amorphous alloys $Al_{80}Fe_{10}M_{10}$ (M = Ni, Ti, V) are one-stage processes, which correspond to the $Al_{13}Fe_4$ intermetallic compounds. The glass forming ability of the Al–Fe–M (M = Ti, V, Ni) ternary systems was evaluated using thermodynamic calculations based on the Miedema model. It was found that the contour maps of the mixing enthalpies depend on the composition and atomic interactions between the elements. According to the experimental results and thermodynamic calculations, the thermal stability of the produced amorphous phase decreases in the order of $Al_{80}Fe_{10}Ti_{10} > Al_{80}Fe_{10}$ $Ni_{10} > Al_{80}Fe_{10}V_{10}$.

Acknowledgement This study was supported by the Green Science Project funded by the Research Institute of Industrial Science and technology (RIST).

References

1. Kim HS, Suryanarayana C, Kim SJ, Chun BS (1998) Powder Metall 41:217
2. Kato H, Yubuta K, Louzguine DV, Inoue A, Kim HS (2004) Scripta Mater 51:577
3. Kiminami CS, Basim ND, Kaufman MJ, Amateau MF, Eden TJ, Galbraith GJ (2001) Key Eng Mater 189/191:503
4. Suryanarayana C (2001) Prog Mater Sci 46:1
5. El-Eskandarany MS, Aoki K, Suzuki K (1997) Scripta Metall Mater 36:1001
6. Portnoy VK, Blinov AM, Tomilin IA, Kuznetsov VN, Kulik T (2002) J Alloy Compd 336:196
7. Kesheng Z, Shengqi X, Jingen Z (2007) Mater Sci Eng A445:48
8. Guang R, Jing-En Z, Shengqi X, Pengliang L (2006) Mater Sci Eng A416:45
9. Matsumoto T (1994) Mater Sci Eng A179/180:511
10. Hong SJ, Kim TS, Kim HS, Kim WT, Chun BS (1999) Mater Sci Eng A271:469
11. Kim HS (2001) Mater Sci Eng A304:327
12. Liu BX, Lai WS, Zhang Q (2000) Mater Sci Eng R29:1
13. Inoue A (1998) Prog Mater Sci 43:365
14. Miedema AR, DeBoer FR, Boom R (1981) Physica B103:67
15. DeBoer FR, Boom R, Mattens WCM, Miedema AR, Niessen AK (2001) Cohesion in metals: transition metal alloy. North-Holland, Amsterdam
16. Niessen AK, DeBoer FR, Boom R, Chatel PF, Mattens WCM, Miedema AR (1983) Calphad 7:51
17. Miedema AR, Chatel PF (1979) In: Proceedings of the symposium theory of alloy phase formation, New Orleans
18. Somoza JA, Gallego LJ, Rey C, Fernandez HM (1992) Phil Mag B65:989
19. Inoue A, Takeuchi A, Shen BL (2001) Mater Trans 42:970
20. Raghavan V (2006) J Phase Equilib Diffus 27:489
21. Grushko B, Lemmerz U, Fischer K, Freiburg C (1996) Phys Stat Sol (a) 155:17